analytical chemistry

Article

pubs.acs.org/ac

Chemical Analysis of Complex Organic Mixtures Using Reactive Nanospray Desorption Electrospray Ionization Mass Spectrometry

Julia Laskin,*[,†] Peter A. Eckert,[‡] Patrick J. Roach,[†] Brandi S. Heath,[‡] Sergey A. Nizkorodov,[§] and Alexander Laskin*[,‡]

[†]Chemical and Materials Sciences Division and [‡]William R. Wiley Environmental and Molecular Sciences Laboratory, Pacific Northwest National Laboratory, P.O. Box 999, MSIN K8-88, Richland, Washington 99352, United States

[§]Department of Chemistry, University of California, Irvine, California 92697-2025, United States

Supporting Information

ABSTRACT: Reactive nanospray desorption electrospray ionization (nano-DESI) combined with high-resolution mass spectrometry was utilized for the analysis of secondary organic aerosol produced through ozonolysis of limonene (LSOA). Previous studies have shown that LSOA constituents are multifunctional compounds containing at least one aldehyde or ketone groups. In this study, we used the selectivity of the Girard's reagent T (GT) toward carbonyl compounds to examine the utility of reactive nano-DESI for the analysis of complex organic mixtures. In these experiments, 1−100 μM GT solutions were used as the working solvents for reactive nano-DESI analysis. Abundant products from the single addition of GT to LSOA constituents were observed at GT concentrations in excess of 10 μM. We found that LSOA dimeric and trimeric compounds react with GT through a simple addition reaction resulting in formation of the carbinolamine derivative. In contrast, reactions of GT with monomeric species result in the formation of both the carbinolamine and the hydrazone derivatives. In addition, several monomers did not react with GT on the time scale of our experiment. These molecules were characterized by relatively high values of the double bond equivalent and low oxygen content. Furthermore, because addition of a charged GT tag to a neutral molecule eliminates the discrimination against the low proton affinity compounds in the ionization process, reactive nano-DESI analysis enables quantification of individual compounds in the complex mixture. For example, we were able to estimate for the first time the amounts of dimers and trimers in the LSOA mixture. Specifically, we found that the most abundant LSOA dimer was detected at the ~0.5 pg level and the total amount of dimers and trimers in the analyzed sample was ~11 pg. Our results indicate that reactive nano-DESI is a valuable approach for examining the presence of specific functional groups and for the quantification of compounds possessing these groups in complex mixtures.

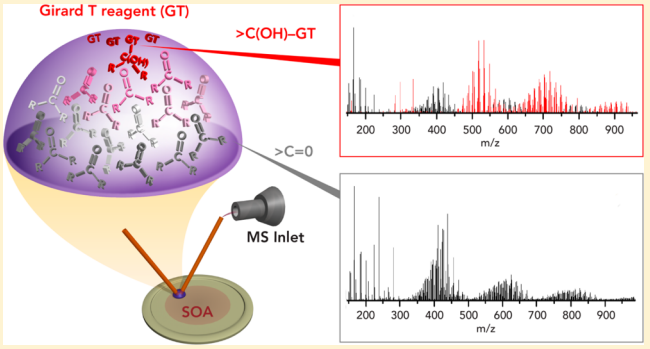

Atmospheric organic aerosol (OA) produced through oxidation of biogenic and anthropogenic volatile organic compounds has a significant impact on human health,[1] climate,[2] and air quality.[3] Chemical characterization of OA using high-resolution mass spectrometry (HR-MS) has recently attracted significant attention[4] because it offers unique insights into complexity and the dynamic nature of OA that undergoes physical and chemical transformations in the atmosphere. Chemical analysis of OA using mass spectrometry typically involves soft ionization of the analyte using, for example, electrospray ionization (ESI)[5] to generate $[M + H]^+$ or $[M + Na]^+$ ions in the positive mode or $[M - H]^-$ ions in the negative mode. Both the mode of ionization (e.g., protonation, deprotonation, and metal complexation) and the ionization efficiency strongly depend on the composition and the structure of the molecule.[6] For example, low proton affinity analytes are rarely observed in positive ESI mass spectra. Significant variations in the ionization efficiencies of analytes result in matrix effects and signal suppression presenting challenges for chemical analysis of complex mixtures using mass spectrometry.[7] In addition, without separation stage, mass spectrometry cannot distinguish isomeric structures. Complementary characterization using liquid chromatography coupled with mass spectrometry (LC/MS) is necessary for detailed characterization of complex mixtures.

Chemical derivatization of analyte molecules is commonly used to alleviate these problems.[6,8,9] The presence of a charged group ensures efficient ionization of analytes of low proton affinity and thereby enables quantification of different classes of molecules in complex mixtures. For example, incorporation of a charged chemical moiety is commonly used for separation,

Received: June 6, 2012
Accepted: July 16, 2012
Published: July 16, 2012

   dx.doi.org/10.1021/ac301533z | Anal. Chem. 2012, 84, 7179−7187

analysis, and quantification of steroids,[10] aldehydes,[11] and oligosaccharides[12] by LC/MS.

Ambient surface ionization enables rapid detection of analytes deposited on substrates without sample preparation.[13−16] When combined with in situ chemical derivatization, these techniques enable sensitive reactive analysis of substrate-deposited analytes that are not readily ionized using soft ionization approaches.[15,17] Reactive analysis has been used in conjunction with ambient surface ionization techniques such as desorption electrospray ionization (DESI),[17−21] electrospray-assisted laser desorption/ionization (ELDI),[22] and laser ablation electrospray ionization (LAESI).[23] For example, chemical derivatization of long-chain alcohols using betaine aldehyde and electrical discharge-induced oxidation was used for detection of saturated hydrocarbons in petroleum samples using reactive DESI.[21] Reactive LAESI was used to generate lithium adducts of lipids for improved structural characterization using MS/MS.[23] Reactive ELDI with disulfide reducing agent was used for direct top-down protein identification.[22]

Our recent studies demonstrated the utility of nanospray desorption electrospray ionization (nano-DESI) for sensitive analysis of complex organic mixtures collected on solid substrates.[24−28] Nano-DESI is an ambient surface ionization technique that relies on the online liquid extraction of analytes from surfaces.[24] In nano-DESI, the analyte is desorbed from the surface into a liquid bridge formed between a primary capillary supplying a solvent to the surface and a nanospray capillary that transfers the dissolved analyte to a mass spectrometer and ionizes the molecules using nanospray ionization. The precise control of desorption and ionization processes enables analysis of OA using less than 10 ng of material.[25] Furthermore, because liquid extraction occurs from a small area of the sample, multiple analyses can be performed on the same OA sample. Here we report a first reactive nano-DESI/HR-MS analysis of laboratory-generated secondary organic aerosol samples produced through ozonolysis of limonene (LSOA). Chemical composition of LSOA has been extensively studied using high-resolution mass spectrometry.[29−32] It has been demonstrated that ozonolysis of limonene and other terpenes produces aerosol that contains a large number of compounds in the m/z 100−1000 range.[31,33−39] Most of these products contain carboxyl, carbonyl, and hydroxyl groups that are not readily ionized as protonated species in the positive mode ESI. In fact, cationization on sodium is the prominent ionization mechanism for LSOA constituents.[31] The complexity of the LSOA sample and the presence of carbonyl compounds make it an excellent model system for reactive analysis.

Previously, we reported on reactive ESI-MS analysis of LSOA using isotopically labeled methanol (CD_3OH) that allowed us to identify carbonyl- and carboxyl-containing LSOA constituents.[40] In this study, we used Girard's reagent T (GT)[41,42] for online reactive nano-DESI analysis of the carbonyl groups in LSOA. Because derivatization of carbonyl compounds using the charged GT reagent converts neutral molecules into positive ions, it is particularly advantageous for subsequent analysis of the derivatized products using ESI. Multiple experiments were performed on the same LSOA sample to examine variations in the composition of the analyte as a function of GT concentration. We demonstrate the utility of this approach for sensitive and quantitative analysis of complex organic mixtures collected on substrates. Furthermore, this approach can be readily extended to other reagents and other functional groups. For example, derivatization of carbonyl compounds through reaction with 2,4-dinitrophenylhydrazone may be used for MS analysis of complex mixtures in the negative mode[43] while the alcohol functional group may be derivatized using betaine aldehyde as a reagent.[20]

EXPERIMENTAL SECTION

Preparation and chemical aging of LSOA was performed as described in our previous studies.[30−32] The detailed procedure is provided in the Supporting Information. Previous studies[29,32] showed that chemical aging of LSOA by reactions with ammonia results in visible browning of the initially white LSOA sample following the formation of light-absorbing nitrogen-containing products. Formation of these species has been attributed to the reactions of ammonia with aldehyde and ketone groups in the LSOA molecules, converting them into primary imines ($R-C{=}NH_2$), secondary imines ($R_1-C{=}NH-R_2$), and other nitrogen-containing compounds.[32]

Both freshly prepared (white) and aged (brown) LSOA samples were analyzed using nano-DESI/HR-MS. High-resolution mass spectra were obtained using a LTQ-Orbitrap mass spectrometer (Thermo Electron, Bremen, Germany) equipped with a commercial DESI source (Prosolia, Inc., Indianapolis, IN) that was modified to accommodate nano-DESI and ESI sources. In these experiments, the sample was positioned on a computer-controlled XYZ stage and brought in contact with the nano-DESI probe. Fused silica capillaries (50 μm i.d., 193 μm o.d., Polymicro Technologies, L.L.C., Phoenix) were used to create the primary and the nanospray capillaries of the probe. The 10−20 mm long nanospray capillary was positioned using a Newport manual MS miniature XYZ stage. Typical experimental conditions were as follows: spray voltage of 3−5 kV, 0.5 mm distance from the tip of the nanospray capillary to the heated inlet of the LTQ-Orbitrap, 250 °C temperature of the heated capillary. The solvent was infused using a syringe pump at a flow rate of 0.3−1 μL/min that was matched to the self-aspiration rate of the nanospray capillary.[24] The mass spectrometer was operated in the positive-ion mode with a resolving power of 60 000 at m/z 412.

The background signal was acquired for 1−2 min by placing the probe on the part of the Teflon substrate that contained no LSOA analyte. The sample was subsequently moved for the analysis of the deposited LSOA material, and the signal was acquired for another 3−4 min. Mass spectra of the sample and the background were subsequently obtained by averaging the signal over the time windows during which the nano-DESI probe was in contact with the LSOA sample and analyte-free area of the substrate, respectively.

Reactive nano-DESI/HR-MS analysis was performed using acetonitrile doped with GT reagent at different concentrations varied in the range of 1−100 μM. No reaction was observed at a GT concentration lower than 1 μM. Multiple analyses at different GT concentrations were performed on the same LSOA material by placing the nano-DESI probe over different areas of the 27 mm diameter sample. The small size of the probe enabled spectral acquisition from ∼15 discrete spots on the sample without returning to already analyzed areas. Data processing was performed as described in our previous studies[44] and detailed in the Supporting Information.

D-limonene (97% purity, Fisher Scientific) and Girard's reagent T (GT), $[(CH_3)_3N^+CH_2C(=O)NHNH_2]Cl^-$ (99% purity, Aldrich), were purchased from Sigma-Aldrich (St. Louis, MO) and used as received.

dx.doi.org/10.1021/ac301533z | Anal. Chem. 2012, 84, 7179−7187

RESULTS AND DISCUSSION

The GT reagent is widely used for extraction of aldehydes and ketones from complex mixtures.[41,42,45,46] GT reacts with carbonyl groups forming water-soluble hydrazones.[45] The reaction proceeds via a two-step mechanism shown below.[47]

$$>C{=}O + H_2N{-}NH{-}C(=O){-}CH_2{-}N^+(CH_3)_3 \rightarrow >C(OH){-}NH{-}NH{-}C(=O){-}CH_2{-}N^+(CH_3)_3 \quad \text{(r1)}$$

$$>C(OH){-}NH{-}NH{-}C(=O){-}CH_2{-}N^+(CH_3)_3 \rightarrow >C{=}N{-}NH{-}C(=O){-}CH_2{-}N^+(-CH_3)_3 + H_2O \quad \text{(r2)}$$

In the first step (reaction r1), addition of GT to the carbonyl group results in formation of a carbinolamine intermediate, which may subsequently undergo dehydration to form a hydrazone (reaction r2). The competition between the rate of formation of carbinolamine and the rate of its dehydration is pH dependent; at low pH the acid-catalyzed dehydration reaction becomes faster than the addition reaction while a stable carbinolamine intermediate is often formed at neutral pH.[46,47] Addition of GT ($C_5H_{14}N_3O^+$) to a neutral molecule, M, through reaction r1 generates an ion with m/z that is 132.1131 higher than the mass of the molecule. However, because mass spectral features of the reactants correspond to either $[M + H]^+$ or $[M + Na]^+$ species, addition of GT results in an m/z shift of either 131.1059 (GT − H) or 109.1239 (GT − Na), respectively. Subsequent loss of H_2O from the carbinolamine intermediate through reaction r2 is associated with overall mass shifts of 113.0953 (GT − H − H_2O) and 91.1134 (GT − Na − H_2O), respectively. We used these characteristic shifts in exact masses to identify the reactant−product pairs produced during reactive nano-DESI analysis of fresh and aged LSOA samples.

Figure 1 shows typical nano-DESI high-resolution mass spectra of LSOA obtained as a function of the GT concentration in the solvent. The spectrum obtained using a 1 μM GT solution contains monomers (i.e., molecules retaining most of the initial skeleton of limonene), dimers, trimers, and tetramers (i.e., monomers covalently bound by ester, hemiacetal, and other linkages) typically observed in LSOA spectra.[31] Products of reaction between GT and LSOA constituents highlighted in red are absent in the 1 μM GT spectrum, but increase gradually with increase in the GT concentration between 5 and 50 μM. As we discuss below, products of both reactions r1 and r2 appear in the nano-DESI mass spectra. Interestingly, dimers, trimers, and tetramers are converted into reaction products almost quantitatively while the fraction of product peaks in the monomeric part of the spectrum obtained even at higher GT concentration (Figure 1d) is significantly smaller. Similar results were obtained for the LSOA sample aged in the presence of NH_3 vapors (see Figure S1 in the Supporting Information).

Time-dependent nano-DESI/HR-MS signal was recorded by placing the probe on the sample and monitoring the signal as a function of time. Figure 2 shows examples of selected ion chronograms (ion signals vs time recorded without chromatographic separation) representing characteristic time-dependent signal of selected m/z features in the 50 μM GT spectrum. Typical time dependence observed for peaks in the monomer region is illustrated in Figure 2a that show chronograms of two

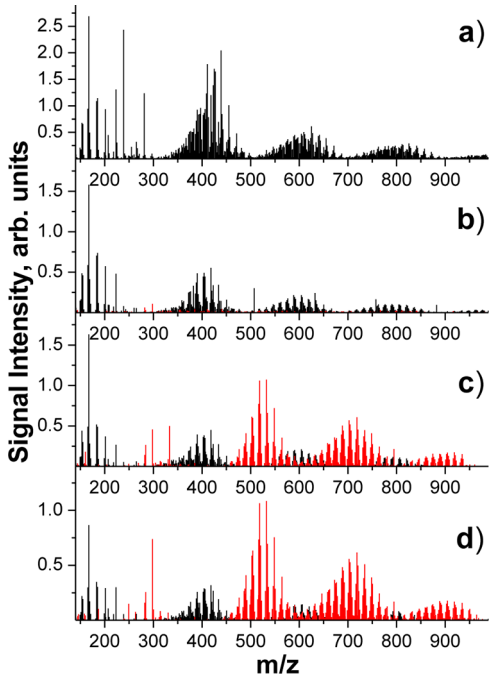

Figure 1. High-resolution nano-DESI spectra of the fresh LSOA material analyzed using a (a) 1 μM, (b) 5 μM, (c) 50 μM, and (d) 100 μM solution of GT in acetonitrile. Peaks corresponding to the products of reaction between LSOA and GT are highlighted in red.

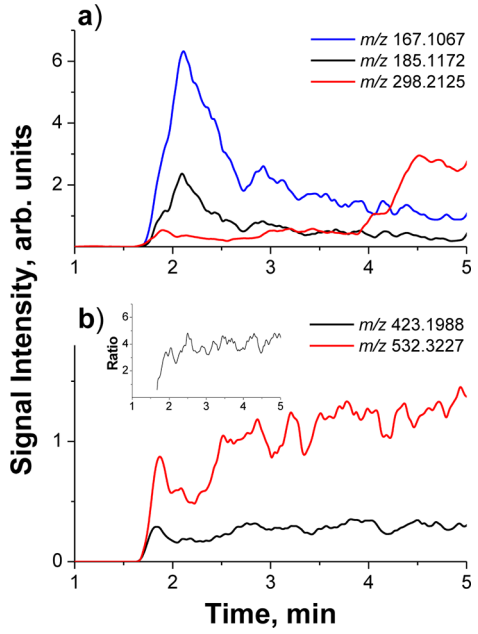

Figure 2. Typical ion chronograms for selected peaks in the (a) monomer and (b) dimer region of the nano-DESI spectrum of the fresh LSOA sample obtained using 50 μM GT in acetonitrile as a solvent. The insert in panel b shows the ratio of the intensities of the product peak at m/z 532.3227 and the reactant peak at m/z 423.1988.

reactant monomer species at m/z 167.1067 and 185.1172 and one product at m/z 298.2125. The signals increase sharply when the nano-DESI probe is placed on the sample (t = 1.65 min). For the reactant molecules, after the initial sharp increase, the signal slowly decreases over the time period of minutes. In contrast, all higher-mass features showed either no change or a very slow increase in the signal as a function of time. For

dx.doi.org/10.1021/ac301533z | Anal. Chem. 2012, 84, 7179−7187

example, Figure 2b shows time-dependent signal obtained for $C_{20}H_{32}O_8Na^+$ at m/z 423.1988, $[M + Na]^+$, and its product of reaction with GT at m/z 532.3227, $[M + GT]^+$. The ratio of the intensities of the product and the reactant shown in the insert shows a rapid increase in the first 0.5 min of the analysis and remains almost constant at longer times. Interestingly, some product signal appears simultaneously with the reactant signal indicating that the reaction is very fast and a majority of the analyte molecules, M, is rapidly converted into $[M + GT]^+$ adducts when the solvent is brought in contact with the LSOA sample. The fast reactivity observed in this study is consistent with the results reported by Girod et al.[48] In that study, the authors observed a dramatic increase in the rate of reaction between GT and analyte molecules in microdroplets as compared to the bulk solution.

Different time dependence of the signals corresponding to the monomeric species as compared to dimers and trimers may be attributed either to the slower kinetics of reaction between the monomers and GT and to faster partitioning of the lower-MW compounds into the solvent during the analysis resulting in faster depletion of the monomer population in the sample. Interestingly, the abundance of the monomeric product at m/z 298.2125 shows a bimodal behavior with a low-abundance product formed through a rapid process once the probe touches the sample and a higher-abundance species formed 2.5 min later. This behavior could be attributed to the presence of multiple pathways and multiple precursor molecules that yield the product at m/z 298.2125.

Figure 3 compares the new peaks corresponding to the products of reaction with GT in both fresh and aged LSOA

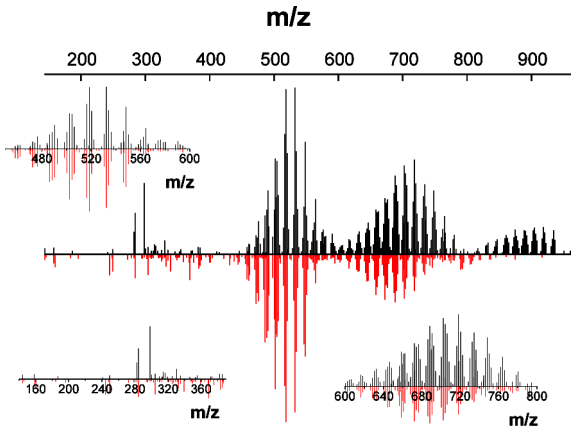

Figure 3. New peaks appearing in the nano-DESI spectra as a result of reactions between GT and the fresh (black) and aged (red) LSOA samples analyzed using 50 μM GT in acetonitrile as a solvent. The insets show expanded views of the regions corresponding to reactions of LSOA monomers, dimers, and trimers.

samples. The data obtained for the aged sample is plotted as negative signal to facilitate the comparison. There is a remarkable overlap between the new peaks observed in the dimer and trimer region of the spectrum. The intensity of the peaks in the tetramer region of the spectrum is often quite low, which contributes to the observed differences between higher-mass species observed in the fresh and aged samples. In the following comparison we will ignore the peaks above m/z 800. We have previously shown[32] that chemical aging of LSOA in the presence of ammonia converts some of the LSOA carbonyl compounds into imines. Detailed peak assignment demonstrated that all GT adducts contained three nitrogen atoms indicating that only $C_xH_yO_z$ compounds in the LSOA samples react with GT ($C_5H_{14}N_3O^+$) on the time scale of our experiment. The absence of peaks corresponding to reactions between GT and the nitrogen-containing species abundant in the aged LSOA sample is responsible for the observed correspondence between the GT products in nano-DESI spectra of the fresh and aged LSOA samples. We also note that we did not observe any doubly charged products corresponding to the addition of two GT molecules to the analyte. The absence of such products may be attributed to the slower kinetics of the subsequent reaction or to the low stability of the doubly charged ions. Because both chemical aging in the presence of NH_3 and reaction with GT target the same functional groups (i.e., carbonyls), we conclude that chemical aging consumes the reactive functional groups necessary for reaction with GT.

The distribution of the products in the reactive nano-DESI mass spectrum may be fully predicted based on the m/z values corresponding to the $C_xH_yO_z$ neutral molecules observed in the LSOA spectra acquired without the GT reagent. Because dimers and trimers are observed mainly as sodiated species, we calculated the predicted distribution of the products of reactions r1 and r2 by adding 109.1240 Da (GT − Na) and 91.1134 Da (GT − Na − H_2O) to the m/z values observed in the spectrum obtained using pure solvent. Figure 4 compares the distribution of the products of reaction with GT obtained by adding 109.1240 (GT − Na, Figure 4a) and 91.1134 Da

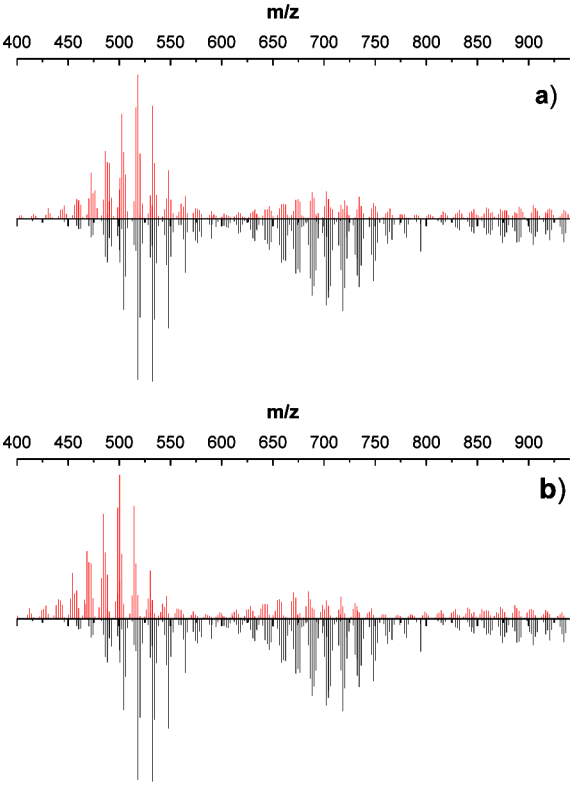

Figure 4. New peaks in the 50 μM GT spectrum of the fresh LSOA sample plotted as negative signal and reaction products of dimers, trimers, and tetramers in the LSOA spectrum predicted by (a) adding the mass of GT and subtracting the mass of Na (no water loss) and (b) adding the mass of GT and subtracting the mass of Na and H_2O shown as positive signal.

dx.doi.org/10.1021/ac301533z | Anal. Chem. 2012, 84, 7179−7187

Table 1. Monomeric LSOA Constituents and the Corresponding Reaction Products Observed Using Reactive nano-DESI Analysis of LSOA with 50 μM GT Solution

m/z	relative abundance, %	$[M + GT]^+$ (131.1059)	$[M + GT - H_2O]^+$ (113.0953)	DBE	neutral formula (M)
		$[M + H]^+$			
153.0911	25.2	284.1969		4	$C_9H_{12}O_2$
155.1067	24.5			3	$C_9H_{14}O_2$
165.091	35.1			5	$C_{10}H_{12}O_2$
167.1066	100.0	298.2125		4	$C_{10}H_{14}O_2$
169.0859	18.4	300.1918		4	$C_9H_{12}O_3$
169.1223	9.0		282.2176	3	$C_{10}H_{16}O_2$
171.1016	6.6	302.2074	284.1969	3	$C_9H_{14}O_3$[a]
183.1015	40.5	314.2074		4	$C_{10}H_{14}O_3$
185.0808	2.7	316.1867		4	$C_9H_{12}O_4$
185.1172	42.6	316.223	298.2125	3	$C_{10}H_{16}O_3$[b]
187.0965	6.3		300.1918	3	$C_9H_{14}O_4$[c]
199.0965	4.6	330.2023	312.1918	4	$C_{10}H_{14}O_4$
201.1121	34.8		314.2074	3	$C_{10}H_{16}O_4$[d]
m/z	relative abundance, %	$[M + GT]^+$ (109.1239)	$[M + GT - H_2O]^+$ (91.1134)	DBE	neutral formula (M)
		$[M + Na]^+$			
207.0991	16.6	316.223	298.2125	3	$C_{10}H_{16}O_3$
209.0574	2.5			8	$C_{12}H_{10}O_2$
209.0784	4.0		300.1918	3	$C_9H_{14}O_4$[c]
223.0731	30.3			8	$C_{13}H_{12}O_2$
223.094	48.6		314.2074	3	$C_{10}H_{16}O_4$
225.0523	11.4			8	$C_{12}H_{10}O_3$
225.1097	1.5		316.223	2	$C_{10}H_{18}O_4$
227.068	1.7			7	$C_{12}H_{12}O_3$
239.068	90.5			8	$C_{13}H_{12}O_3$
239.089	2.2		330.2023	3	$C_{10}H_{16}O_5$

Tracers of limonene ozonolysis highlighted in the table: [a]keto-limonaldedyde, [b]limononic acid, [c]limonic acid, [d]7OH-limononic acid. See ref 31 for detailed assignments.

(GT − Na − H_2O, Figure 4b) to the observed m/z values of dimers and trimers in the LSOA spectrum with the new peaks observed in the 50 μM GT spectrum of fresh LSOA (shown as a negative signal). The predicted and observed distributions shown in Figure 4a are remarkably similar. However, the match between the observed distribution of products and the predicted distribution obtained by adding 91.1134 Da (GT − Na − H_2O) shown in Figure 4b is not as good. These results indicate that most dimers and trimers react with GT without the concomitant loss of H_2O from the carbinolamine. Interestingly, previous work[20] showed the exclusive formation of the hydrazone during reaction of cholesterol with GT. The high yield of the products of reaction r1 observed in this study is most likely related to the pH of the solution. We note that no acid was added to the GT solution and the LSOA extract is typically only weakly acidic.

In contrast, there is a significant difference between the types of products observed in the monomer regions of the spectra. Table 1 and Table S1 in the Supporting Information list abundant $[M + H]^+$ and $[M + Na]^+$ ions in the monomer region of the spectrum and the m/z values of the peaks that may be attributed to reactions with GT. We note that several precursor molecules may result in formation of the same product ion. For example, the peak at m/z 298.2125 may be a product of the GT addition to $C_{10}H_{14}O_2$ (m/z 167.1066) without the concomitant water loss or hydrazone formation (reaction r2) from $C_{10}H_{16}O_3$ (m/z 185.1172 for $[M + H]^+$ and 207.0991 for $[M + Na]^+$). It is impossible to distinguish between these reactions based on the accurate mass measurement. Reaction r2 is more likely because several major identified products of limonene ozonolysis have the formula $C_{10}H_{16}O_3$ (e.g., limononic acid and 7-hydroxy-limononaldehyde).[49] However, products with formula $C_{10}H_{14}O_2$ are also produced under high concentration conditions via OH loss from the Criegee intermediates, followed by self-reactions of alkyl peroxy radiacals (see the Supporting Information of ref 31). Therefore, it is likely that both reactions r1 and r2 may contribute to the abundance of the product at m/z 298.2125. More detailed characterization of such products would require coupling reactive nano-DESI with chromatographic separation.

Detailed examination of the data shown in Table 1 and Table S1 in the Supporting Information indicates that some monomeric species do not have a corresponding product of its reaction with GT detected in the spectrum. Most unreactive molecules are characterized by high DBE values (DBE ≥ 5) and contain only 2−3 oxygen atoms. Identification of these molecules is beyond the scope of this paper. Other studies examined the formation of high DBE aromatic products formed during oxidation of terpenes.[30,50,51] Johnston and co-workers suggested that dehydration of alcohols may be responsible for the formation of such species.[50]

Monomers observed as $[M + Na]^+$ ions predominantly form hydrazone products $[M + GT - H_2O]^+$, while molecules observed as protonated species in the LSOA spectrum show both carbinolamine $[M + GT]^+$ and hydrazone $[M + GT - H_2O]^+$ products (Table S1 in the Supporting Information). We have previously demonstrated that the major LSOA constituents observed as $[M + Na]^+$ ions commonly contain reactive aldehyde groups.[40] Because of the higher reactivity of the aldehyde group as compared to the ketone group, we

dx.doi.org/10.1021/ac301533z | Anal. Chem. 2012, 84, 7179−7187

hypothesize that LSOA species containing aldehyde groups form hydrazone product upon reaction with the GT, while molecules containing ketone groups may form either hydrazone or carbinolamine products. This assertion is consistent with the observed reactivity of dimers and trimers. Indeed, aldehyde groups are consumed during the formation of oligomeric species in LSOA via hemiacetal mechanism[30] making them less abundant in dimers and trimers as compared to monomers.

On the basis of the above discussion, we established precursor−product relationships for dimers and trimers that undergo almost exclusive formation of carbinolamine products via reaction r1. Figure 5 shows the dependence of the yield of

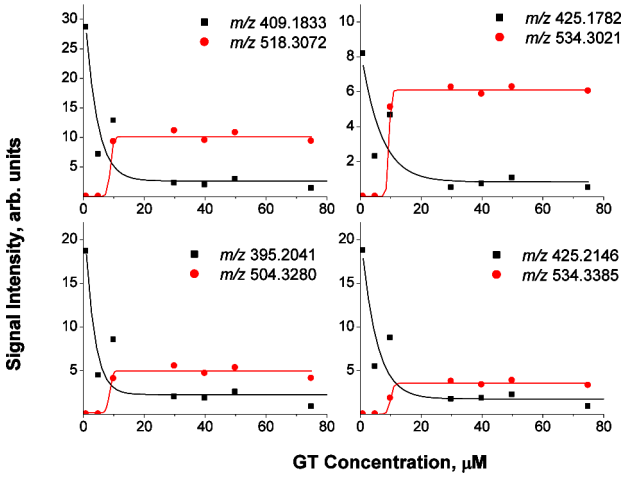

Figure 5. The dependence of signal intensities of selected reactant (black squares) and product (red circles) peaks on the GT concentration.

several carbinolamine products on the GT concentration along with the corresponding precursor molecules. As mentioned earlier, no product ions were observed at 1 μM GT concentration. The signals of the $[M + GT]^+$ products increase rapidly when the GT concentration increases from 5 to 10 μM and reach saturation above a ∼10 μM concentration of the reagent. We also observe a corresponding decrease in the $[M + Na]^+$ reactant signals when the GT concentration increases from 1 to 5 μM, which may be related to the reactant consumption but most likely is additionally affected by signal suppression during the ionization process as we discuss below.

The initial concentration of the reactants can be estimated assuming that there is no signal suppression during the ionization process and assuming uniform ionization efficiency for the GT^+ and the $[M + GT]^+$ products. The second assumption is reasonable because all $[M + GT]^+$ products are preformed ions in solution, for which the ionization efficiency is only affected by the surface activity of the molecules. However, the first assumption requires additional justification. Figure 6 shows the dependence of the total ion signal, the signal of the GT^+, and the total ion signal excluding the abundance of the GT peak at m/z 132.1131 on the GT concentration. The total signal remains fairly constant within ∼25% acceptable variation. However, because at higher GT concentrations a significant fraction of the total ion signal corresponds to the GT abundance, we observe a decrease in the signal of the LSOA constituents with an increase in the GT concentration. It follows that there is a measurable suppression (a factor of ∼2.2) of the LSOA signal at higher GT concentrations.

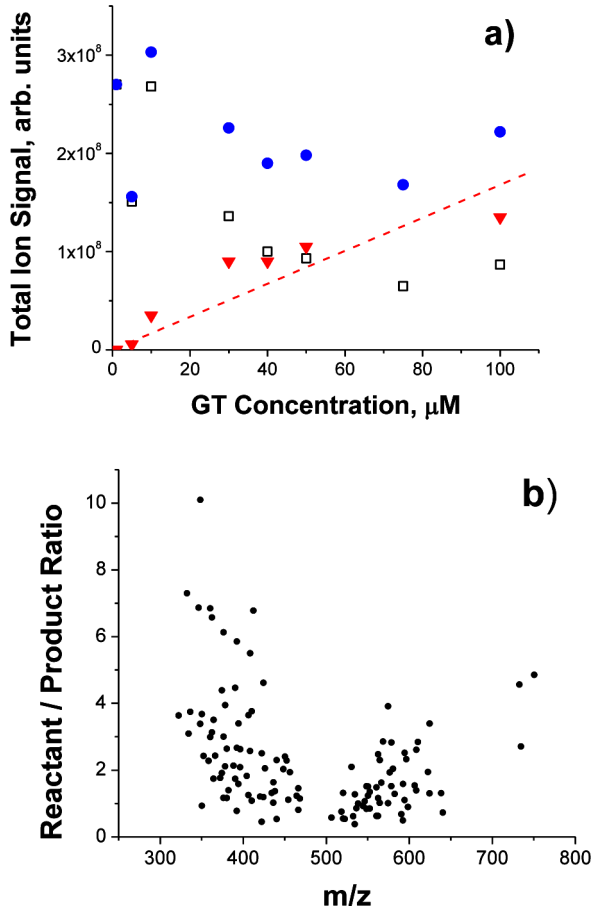

Figure 6. (a) Total ion signal in nano-DESI spectra obtained at different GT concentrations. Blue circles correspond to the total ion signal that includes the GT peak at m/z 132.1131; black squares correspond to the total ion signal that does not include the GT peak; red triangles correspond to the GT signal at m/z 132.1131. The dashed line shows the linear fit for the GT signal with a slope of 1.7×10^6. (b) Ratio of the abundances of reactant and product peaks in the dimer and trimer region of the spectrum as a function of m/z.

The observed signal suppression is further examined in Figure 6b, in which the ratio of intensities of $[M + Na]^+$ reactants detected in the 1 μM GT spectrum and the corresponding $[M + GT]^+$ products in the 50 μM GT spectrum is plotted as a function of m/z. Although the values range from 0.36 to 10, the majority of data points are close to 2 and the ratio shows no obvious dependence on m/z. The average reactant-to-product ratio of 2.3 ± 1.7 is consistent with the observed drop of the total ion signal shown in Figure 6a. The decreased abundance of the $[M + GT]^+$ products as compared to the $[M + Na]^+$ reactants is surprising. Because GT converts neutral molecules into ions, we expected that the $[M + GT]^+$ products should be more abundant than the corresponding $[M + Na]^+$ precursors. On the basis of the above discussion, we conclude that addition of GT to the solvent results in suppression of the LSOA signals in the dimer and trimer region by at least a factor of 2, without an obvious dependence on m/z.

Figure 6a shows the dependence of the measured GT signal at m/z 132.1311 on the GT concentration in solution. As expected, the GT signal shows a gradual increase with concentration. Although the observed trend is not linear, the ionization efficiency can be estimated to within a factor of 2

dx.doi.org/10.1021/ac301533z | Anal. Chem. 2012, 84, 7179−7187

Table 2. Quantification of the Most Abundant $[M + GT]^+$ Species in Reactive Nano-DESI Spectra of LSOA

peak assignment	m/z	ion signal, arb. units	effective concentration, μM	amount of material, mol	amount of material, pg
$C_{19}H_{30}O_8 + C_5H_{14}N_3O^+$	518.3072	1.1×10^6	0.66	4.3×10^{-16}	0.17
$C_{20}H_{32}O_8 + C_5H_{14}N_3O^+$	532.3229	1.1×10^6	0.64	4.2×10^{-16}	0.17
$C_{20}H_{32}O_7 + C_5H_{14}N_3O^+$	516.3280	8.5×10^5	0.50	3.3×10^{-16}	0.12
$C_{19}H_{30}O_7 + C_5H_{14}N_3O^+$	502.3123	8.8×10^5	0.52	3.4×10^{-16}	0.12
$C_{19}H_{30}O_9 + C_5H_{14}N_3O^+$	534.3021	6.8×10^5	0.40	2.6×10^{-16}	0.10
$C_{18}H_{26}O_8 + C_5H_{14}N_3O^+$	502.2761	1.9×10^5	0.11	7.3×10^{-17}	0.03

using a linear fit shown in the figure. The concentration of the analyte molecules can be estimated from the flat part of the concentration-dependent profiles of the $[M + GT]^+$ product ions, some of which are shown in Figure 5. When GT is supplied in excess, the final concentrations of the $[M + GT]^+$ products are equal to the corresponding concentrations of the analyte molecules, M, consumed in the reaction. The final concentrations of the products were derived from the observed signal intensities of $[M + GT]^+$ species in the plateau region of the plots shown in Figure 5. The observed signal intensities for several abundant $[M + GT]^+$ adducts are summarized in Table 2. Assuming the ionization efficiency is uniform for GT^+ and its $[M + GT]^+$ adducts, the concentration of the $[M + GT]^+$ adducts is given by the ratio of the signal intensity in the plateau region divided by the ionization efficiency of GT. The effective ionization efficiency of $1.7 \times 10^6\ \mu M^{-1}$ is derived from the plot shown in Figure 6a. Using this value, we estimated the signal observed for the most abundant $[M + GT]^+$ peak at m/z 518.3072 produced from the analyte $C_{19}H_{30}O_8$ molecule corresponds to an effective concentration of 0.66 μM in the droplet. On the basis of the flow rate of 0.8 μL/min and the typical accumulation time in the LTQ of 50 ms, we estimate that this corresponds to effectively detecting 0.66 $\mu M \times 1.3 \times 10^{-2}\ \mu L/s \times 0.05$ s $= 4.3 \times 10^{-16}$ mol of the analyte molecules per scan. Using the molecular weight of the precursor molecule of 386.1935 g/mol, we estimate the observed signal corresponds to ~0.17 pg of the single most abundant LSOA dimer in the complex mixture. By summing up all the abundances of the observed products we estimate the total mass of the analyzed material is ~5 pg. Taking into account the estimated signal suppression upon addition of GT to the solvent by a factor of 2.2 as discussed earlier, we obtain somewhat higher values of ~0.5 and 11 pg, respectively.

An independent estimation of the amount of the analyzed material is obtained from the known mass of the LSOA material deposited on the substrate and the area of the spot analyzed by nano-DESI. In our experiments, the total mass of LSOA of ~80 μg was deposited onto a 27 mm in diameter circular spot on the substrate, while nano-DESI signal was collected from a ~2 mm spot on the substrate, which contained ~0.4 μg of the LSOA material. Because the signal from one spot lasted for ~5 min and the average accumulation time in the LTQ was 0.05 s/spectrum, the signal observed in each spectrum corresponds to 0.4 $\mu g \times 0.05$ s/300 s = 64 pg of material. We note that the total amount of material consumed in nano-DESI is significantly larger than this value. Specifically, more than 1 ng of material is consumed during the 1.66 s necessary for acquisition of a single LTQ/Orbitrap spectrum with 60 000 resolution. However, because of the low duty cycle of the signal acquisition (short accumulation in the LTQ trap followed by much longer FT analysis in the Orbitrap), most of this material does not contribute to the observed ion abundance.

Despite all the approximations involved in the above estimations and taking into account that not all molecules in the complex LSOA sample react with GT, the results obtained using the two different estimation approaches described above are strikingly similar. It follows that reactive nano-DESI described in this study can be used for semiquantitative analysis of individual components of complex mixtures. This is a significant finding because of the inherent difficulties associated with quantification of large molecules in complex mixtures such as OA. Although GT is only reactive toward carbonyl groups in OA samples, alternative reagents could be identified and used in future studies for targeted quantitative characterization of individual constituents in laboratory and field-collected samples of OA and other environmental organics.

CONCLUSIONS

In this study, we demonstrated efficient online chemical derivatization of the constituents of a complex LSOA mixture using reactive nano-DESI analysis. The analysis was performed by adding varying amounts of the charged GT reagent to the solvent. Because of the small size of the nano-DESI probe, we were able to perform multiple analyses on the same LSOA sample without returning to already analyzed areas. This approach reduces the time required for preparation and collection of the LSOA and significantly enhances the reproducibility of the reactive nano-DESI spectra, which is critical for studying the effect of the reagent concentration on the observed product distribution.

Reactive analysis using GT as a reagent is targeted toward aldehydes and ketones, the classes of compounds that are not readily ionized as protonated species. Addition of a charged tag to these compounds results in a more uniform ionization and eliminates discrimination against low proton affinity species. Using high-resolution mass spectrometry, we examined the effect of GT concentration on the product distribution. Efficient product formation was observed at GT concentrations between 10 and 100 μM. The product species were formed almost immediately after the nano-DESI probe was placed on the LSOA sample indicating fast reaction kinetics. Interestingly, reactive analysis of the fresh and chemically aged LSOA samples resulted in almost identical product distributions indicating that the products of chemical aging present in the aged LSOA sample are not reactive toward GT.

Comparison between the predicted and observed product distributions indicated that oligomeric species in the LSOA sample react with GT via an addition reaction without concomitant loss of water while the monomeric species may form either carbonolamine (reaction r1) or hydrazone product (reaction r2). We hypothesize that the presence of aldehyde groups in the monomeric species facilitates hydrazone formation while ketone groups abundant in the oligomeric species form carbonolamine derivatives. Because the kinetics of

dx.doi.org/10.1021/ac301533z | Anal. Chem. 2012, 84, 7179−7187

the dehydration reaction is pH dependent, the observed product distribution may be affected by the experimental conditions (e.g., pH of the solvent and the overall composition of the sample).

We also demonstrated the utility of reactive nano-DESI for quantification of individual constituents in a complex mixture without an internal standard. Because of the signal suppression in the ionization process, the accuracy of quantification is not very high. Nevertheless this approach can be used to estimate concentrations of individual molecules to within an order of magnitude in complex mixtures that cannot be quantified using the existing analytical approaches. Although in this study we used GT as a reagent, this approach can be readily extended to other charged reagents.

■ ASSOCIATED CONTENT

Ⓢ Supporting Information

Experimental details, complete Table 1, and high-resolution nano-DESI spectra of the aged LSOA material. This material is available free of charge via the Internet at http://pubs.acs.org.

■ AUTHOR INFORMATION

Corresponding Author

*E-mail: Julia.Laskin@pnnl.gov (J.L.); Alexander.Laskin@pnnl.gov (A.L.).

Notes

The authors declare no competing financial interest.

■ ACKNOWLEDGMENTS

The research presented here was performed at EMSL, a national scientific user facility sponsored by the U.S. Department of Energy's (U.S. DOE) Office of Biological and Environmental Research and located at the Pacific Northwest National Laboratory (PNNL). PNNL is operated by Battelle for the U.S. DOE. J.L. and P.J.R. acknowledge support from the DOE's Office of Basic Energy Sciences, Division of Chemical Sciences, Geosciences & Biosciences. A.L. acknowledges support from the EMSL Intramural Program. P.A.E. and B.S.H. acknowledge support from the DOE Science Undergraduate Laboratory Internship Program. S.A.N. was supported by NSF Grant CHE-0909227.

■ REFERENCES

(1) Mauderly, J. L.; Chow, J. C. *Inhalation Toxicol.* **2008**, *20*, 257–288.

(2) Chin, M.; Kahn, R. A.; Schwartz, S. E., *Atmospheric Aerosol Properties and Climate Impacts*; Aeronautics and Space Administration: Washington, DC, 2009; p 115.

(3) Menon, S.; Unger, N.; Koch, D.; Francis, J.; Garrett, T.; Sednev, I.; Shindell, D.; Streets, D. *Environ. Res. Lett.* **2008**, *3*, 024004 (12 pages).

(4) Nizkorodov, S. A.; Laskin, J.; Laskin, A. *Phys. Chem. Chem. Phys.* **2011**, *13*, 3612–3629.

(5) Fenn, J. B.; Mann, M.; Meng, C. K.; Wong, S. F.; Whitehouse, C. M. *Science* **1989**, *246*, 64–71.

(6) Cech, N. B.; Enke, C. G. *Mass Spectrom. Rev.* **2001**, *20*, 362–387.

(7) Enke, C. G. *Anal. Chem.* **1997**, *69*, 4885–4893.

(8) Xu, F. G.; Zou, L.; Liu, Y.; Zhang, Z. J.; Ong, C. N. *Mass Spectrom. Rev.* **2011**, *30*, 1143–1172.

(9) Quirke, J. M. E.; Adams, C. L.; Vanberkel, G. J. *Anal. Chem.* **1994**, *66*, 1302–1315.

(10) Higashi, T.; Shimada, K. *Anal. Bioanal. Chem.* **2004**, *378*, 875–882.

(11) Eggink, M.; Wijtmans, M.; Ekkebus, R.; Lingeman, H.; de Esch, I. J. P.; Kool, J.; Niessen, W. M. A.; Irth, H. *Anal. Chem.* **2008**, *80*, 9042–9051.

(12) Unterieser, I.; Mischnick, P. *Carbohydr. Res.* **2011**, *346*, 68–75.

(13) Ifa, D. R.; Jackson, A. U.; Paglia, G.; Cooks, R. G. *Anal. Bioanal. Chem.* **2009**, *394*, 1995–2008.

(14) Van Berkel, G. J.; Pasilis, S. P.; Ovchinnikova, O. *J. Mass Spectrom.* **2008**, *43*, 1161–1180.

(15) Cooks, R. G.; Ouyang, Z.; Takats, Z.; Wiseman, J. M. *Science* **2006**, *311*, 1566–1570.

(16) Harris, G. A.; Galhena, A. S.; Fernandez, F. M. *Anal. Chem.* **2011**, *83*, 4508–4538.

(17) Chen, H.; Talaty, N. N.; Takáts, Z.; Cooks, R. G. *Anal. Chem.* **2005**, *77*, 6915–6927.

(18) Chen, H.; Cotte-Rodriguez, I.; Cooks, R. G. *Chem. Commun.* **2006**, 597–599.

(19) Huang, G.; Chen, H.; Zhang, X.; Cooks, R. G.; Ouyang, Z. *Anal. Chem.* **2007**, *79*, 8327–8332.

(20) Wu, C. P.; Ifa, D. R.; Manicke, N. E.; Cooks, R. G. *Anal. Chem.* **2009**, *81*, 7618–7624.

(21) Wu, C. P.; Qian, K. N.; Nefliu, M.; Cooks, R. G. *J. Am. Soc. Mass Spectrom.* **2010**, *21*, 261–267.

(22) Peng, I. X.; Loo, R. R. O.; Shiea, J.; Loo, J. A. *Anal. Chem.* **2008**, *80*, 6995–7003.

(23) Shrestha, B.; Nemes, P.; Nazarian, J.; Hathout, Y.; Hoffman, E. P.; Vertes, A. *Analyst* **2010**, *135*, 751–758.

(24) Roach, P. J.; Laskin, J.; Laskin, A. *Analyst* **2010**, *135*, 2233–2236.

(25) Roach, P. J.; Laskin, J.; Laskin, A. *Anal. Chem.* **2010**, *82*, 7979–7986.

(26) Nguyen, T. B.; Roach, P. J.; Laskin, J.; Laskin, A.; Nizkorodov, S. A. *Atmos. Chem. Phys.* **2011**, *11*, 6931–6944.

(27) Laskin, J.; Heath, B. S.; Roach, P. J.; Cazares, L.; Semmes, O. J. *Anal. Chem.* **2012**, *84*, 141–148.

(28) Eckert, P. A.; Roach, P. J.; Laskin, A.; Laskin, J. *Anal. Chem.* **2012**, *84*, 1517–1525.

(29) Bones, D. L.; Henricksen, D. K.; Mang, S. A.; Gonsior, M.; Bateman, A. P.; Nguyen, T. B.; Cooper, W. J.; Nizkorodov, S. A. *J. Geophys. Res.-Atmos.* **2010**, 115.

(30) Bateman, A. P.; Nizkorodov, S. A.; Laskin, J.; Laskin, A. *Phys. Chem. Chem. Phys.* **2009**, *11*, 7931–7942.

(31) Walser, M. L.; Desyaterik, Y.; Laskin, J.; Laskin, A.; Nizkorodov, S. A. *Phys. Chem. Chem. Phys.* **2008**, *10*, 1009–1022.

(32) Laskin, J.; Laskin, A.; Roach, P. J.; Slysz, G. W.; Anderson, G. A.; Nizkorodov, S. A.; Bones, D. L.; Nguyen, L. Q. *Anal. Chem.* **2010**, *82*, 2048–2058.

(33) Tolocka, M. P.; Jang, M.; Ginter, J. M.; Cox, F. J.; Kamens, R. M.; Johnston, M. V. *Environ. Sci. Technol.* **2004**, *38*, 1428–1434.

(34) Gao, S.; Keywood, M.; Ng, N. L.; Surratt, J.; Varutbangkul, V.; Bahreini, R.; Flagan, R. C.; Seinfeld, J. H. *J. Phys. Chem. A* **2004**, *108*, 10147–10164.

(35) Muller, L.; Reinnig, M. C.; Warnke, J.; Hoffmann, T. *Atmos. Chem. Phys.* **2008**, *8*, 1423–1433.

(36) Yasmeen, F.; Vermeylen, R.; Szmigielski, R.; Iinuma, Y.; Boge, O.; Herrmann, H.; Maenhaut, W.; Claeys, M. *Atmos. Chem. Phys.* **2010**, *10*, 9383–9392.

(37) Nguyen, T. B.; Bateman, A. P.; Bones, D. L.; Nizkorodov, S. A.; Laskin, J.; Laskin, A. *Atmos. Environ.* **2010**, *44*, 1032–1042.

(38) Hall, W. A.; Johnston, M. V. *Aerosol Sci. Technol.* **2011**, *45*, 37–45.

(39) Hall, W. A.; Johnston, M. V. *J. Am. Soc. Mass Spectrom.* **2012**, *23*, 1097–1108.

(40) Bateman, A. P.; Walser, M. L.; Desyaterik, Y.; Laskin, J.; Laskin, A.; Nizkorodov, S. A. *Environ. Sci. Technol.* **2008**, *42*, 7341–7346.

(41) Teitelbaum, C. L. *J. Org. Chem.* **1958**, *23*, 646–647.

(42) Wheeler, O. H. *Chem. Rev.* **1962**, *62*, 205.

(43) Brombacher, S.; Oehme, M.; Beukes, J. A. *J. Environ. Monit.* **2001**, *3*, 311–316.

(44) Roach, P. J.; Laskin, J.; Laskin, A. *Anal. Chem.* **2011**, *83*, 4924−4929.
(45) Gaddis, A. M.; Ellis, R.; Currie, G. T. *Nature* **1961**, *191*, 1391.
(46) Mitchel, R. E. J.; Birnboim, H. C. *Anal. Biochem.* **1977**, *81*, 47−56.
(47) Stachissini, A. S.; Doamaral, L. *J. Org. Chem.* **1991**, *56*, 1419−1424.
(48) Girod, M.; Moyano, E.; Campbell, D. I.; Cooks, R. G. *Chem. Sci.* **2011**, *2*, 501−510.
(49) Leungsakul, S.; Jaoui, M.; Kamens, R. M. *Environ. Sci. Technol.* **2005**, *39*, 9583−9594.
(50) Heaton, K. J.; Sleighter, R. L.; Hatcher, P. G.; Hall, W. A., IV; Johnston, M. V. *Environ. Sci. Technol.* **2009**, *43*, 7797−7802.
(51) Gratien, A.; Johnson, S. N.; Ezell, M. J.; Dawson, M. L.; Bennett, R.; Finlayson-Pitts, B. J. *Environ. Sci. Technol.* **2011**, *45*, 2755−2760.